Journal of Informatics and Mathematical Sciences
Vol. 10, Nos. 1 & 2, pp. 371–381, 2018
ISSN 0975-5748 (online); 0974-875X (print)
Published by RGN Publications

http://www.rgnpublications.com

http://dx.doi.org/10.26713/jims.v10i1-2.1069

Research Article

Natural Convection Flow of Nanofluids in Squeeze Film with an Exponential Curvature

Vimala P.* and Manimegalai K.

Department of Mathematics, Anna University, Chennai, India
***Corresponding author:** vimalapon7@gmail.com

Abstract. A theoretical study of the laminar squeeze flow of copper water and alumina water nanofluids between a flat circular stationary disk and a curved circular moving disk is carried out using energy integral method. The squeeze film behaviour is examined analytically and the effects of inertia and curvature on the squeeze film pressure, load carrying capacity of the fluid and temperature are analysed. Further, the problem is solved numerically for a sinusoidal motion of the upper curved disk taking an exponential form of the gap width. It is found that the copper water nanofluid is better than alumina water nanofluid for better heat transfer rates. While high inertia forces strongly influence the squeeze film behaviour, low inertia forces are favourable for temperature distribution. Further, concave nature of the upper disk gives better squeeze film characteristics than convex disk. However, convex disk is better than concave disk as far as the temperature distribution is concerned.

Keywords. Hydrodynamic lubrication; Nanofluids; Curved squeeze films; Inertial effects; Thermal effects

MSC. 35Q35; 76D08; 82D80

Received: October 13, 2017 **Accepted:** December 29, 2017

This article was submitted to “National Conference on Fluid Mechanics (NCFM 2017)” organized by SSN College of Engineering (Anna University), Chennai, India during October 27-28, 2017.

1. Introduction

Squeeze films are encountered enormously in applications such as hydrodynamic lubrication, turbo-machinery, automotive engines, etc. There are many applications involving squeeze films in curved circular geometries. Thus many authors have investigated the combined effects of curvature and inertia on the squeeze film behaviour [7, 11, 12, 13, 14]. In addition, thermal effects on the squeeze film characteristics have also been considered in literature [4, 10].

Nanofluids are suspensions involving a base fluid containing nanoparticles. They have many possible applications like solar energy absorption and friction reduction used in automobile brake fluids. They also find applications in drug delivery, microelectronics, defense, nuclear systems, space craft, etc. The efficiency of heat transfer in boundary layer flow and squeeze film flows involving nanofluids have been studied by many researchers [1, 5, 8].

The present problem studies the combined effects of inertia and curvature on squeeze film behaviour of nanofluids between a flat circular stationary disk and a curved circular moving disk. The solution is obtained for the sinusoidal motion of the exponential curved disk using energy integral method. Also the variations in squeeze film pressure, squeeze film force and mean temperature distribution for copper water and alumina water nanofluids, with different volume fractions, are analysed.

Section 2 presents the mathematical formulation for the problem. Section 3 describes the solution by energy integral method. Section 4 elaborates on the results and discussion of the problem. Section 5 gives the conclusion drawn from the present investigation.

2. Mathematical Formulation

The laminar squeeze flow of an incompressible viscous nanofluid between a flat circular stationary disk at $z = 0$ and a curved circular moving disk at $z = h(r,t)$ is considered (Figure 1). The upper curved circular disk of radius r_a approaches the lower flat circular disk with a squeezing velocity of $-h_t(r,t)$ (or) $-\frac{\partial h(r,t)}{\partial t}$, where r is the radial coordinate and t is the time. The temperatures on the lower and upper disks are taken to be θ_0 and θ_1, respectively. Here u and w are the velocity components in radial and axial directions, respectively.

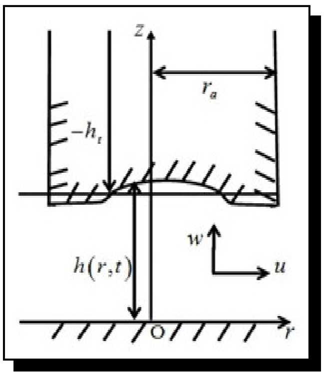

Figure 1. Curved squeeze film geometry

The flow is assumed to be axisymmetric and laminar and the body forces are absent. Under these hydrodynamic lubrication assumptions the governing equations in the non-dimensional form are given by

$$\frac{1}{R}\frac{\partial(RU)}{\partial R} + \frac{\partial W}{\partial Z} = 0, \tag{2.1}$$

$$Re\left(\frac{\partial U}{\partial T} + U\frac{\partial U}{\partial R} + W\frac{\partial U}{\partial Z}\right) = -\frac{\partial P}{\partial R} + \frac{\partial^2 U}{\partial Z^2}, \tag{2.2}$$

$$\frac{\partial P}{\partial Z}=0, \tag{2.3}$$

$$RePr\left(\frac{\partial\Theta}{\partial T}+U\frac{\partial\Theta}{\partial R}+W\frac{\partial\Theta}{\partial Z}\right)=\frac{\partial^2\Theta}{\partial Z^2}+EcPr\left(\frac{\partial U}{\partial Z}\right)^2 \tag{2.4}$$

along with the boundary conditions for velocity components, pressure and temperature given by

$$U=0,\ W=0 \text{ on } Z=0;\ \ U=0,\ W=\frac{\partial H(R,T)}{\partial T} \text{ on } Z=H(R,T), \tag{2.5}$$

$$\frac{\partial P}{\partial R}=0 \text{ on } R=0;\ \ P=0 \text{ on } R=1, \tag{2.6}$$

$$\Theta=1 \text{ on } Z=0, \tag{2.7}$$

$$\frac{\partial\Theta}{\partial Z}=0 \text{ on } Z=H(R,T). \tag{2.8}$$

The integral form of the continuity equation in the non-dimensional form and the mean temperature are given by

$$\int_0^{H(R,\,T)}U\,dZ=-\frac{1}{R}\int_0^R R\frac{\partial H(R,T)}{\partial T}dR, \tag{2.9}$$

$$\frac{1}{H}\int_0^{H(R,T)}\Theta dZ=\Theta_m. \tag{2.10}$$

Equations (2.1)-(2.10) have been obtaining by using the following non-dimensional quantities

$$R=\frac{r}{r_a},\ Z=\frac{z}{h_0},\ H=\frac{h}{h_0},\ T=\omega t,\ U=\frac{u}{\omega r_a},\ W=\frac{w}{\omega h_0},\ \Theta=\frac{\theta-\theta_1}{\theta_0-\theta_1},\ P=\frac{p{h_0}^2}{\mu_{nf}{r_a}^2\omega}$$

$$Re=\frac{\rho_{nf}\omega {h_0}^2}{\mu_{nf}},\ Pr=\frac{(\mu C_P)_{nf}}{k_{nf}},\ Ec=\frac{\omega^2{r_a}^2}{(C_P)_{nf}(\theta_0-\theta_1)}, \tag{2.11}$$

where P is the pressure, Θ is the temperature, ρ_{nf} is the density, μ_{nf} is the dynamic viscosity, $(C_P)_{nf}$ is the specific heat capacity and k_{nf} is the thermal conductivity of the nanofluid.

3. Solution by Energy Integral Method (EIM)

The velocity components U, W, pressure P and mean temperature Θ_m are obtained using equations (2.1)-(2.10) by energy integral method. Multiplying equation (2.2) by U on both sides and integrating from $Z=0$ to $Z=H(R,T)$ and using equations (2.1), (2.2) and (2.5), gives

$$Re\left(\frac{\partial}{\partial T}\int_0^{H(R,T)}\left(\frac{U^2}{2}\right)dZ+\frac{1}{2}\frac{\partial}{\partial R}\int_0^{H(R,T)}U^3dZ+\frac{1}{2R}\int_0^{H(R,T)}U^3dZ\right)$$
$$=-\frac{\partial P}{\partial R}\int_0^{H(R,T)}UdZ+\int_0^{H(R,T)}U\frac{\partial^2U}{\partial Z^2}dZ. \tag{3.1}$$

The inertialess solution of radial velocity component U obtained from equation (3.1) using equation (2.9) with the boundary conditions (2.5) is given by

$$U=\frac{6}{RH^3}\left(\int_0^R R\frac{\partial H}{\partial T}dR\right)(Z^2-HZ). \tag{3.2}$$

Using equation (3.2) in continuity equation (2.1), the axial velocity component W is obtained as

$$W=\frac{18H_R}{RH^4}\left(\frac{Z^3}{3}-\frac{HZ^2}{2}\right)\int_0^R R\frac{\partial H}{\partial T}dR-\frac{6}{H^3}\frac{\partial H}{\partial T}\left(\frac{Z^3}{3}-\frac{HZ^2}{2}\right)+\frac{3H_RZ^2}{RH^3}\int_0^R R\frac{\partial H}{\partial T}dR. \tag{3.3}$$

Using equation (3.2) in (3.1), the pressure gradient is obtained which on integration yields the pressure distribution as

$$\begin{aligned} P = &-12\int_R^1 \frac{1}{RH^3}\left(\int_0^R R\frac{\partial H}{\partial T}dR\right)dR \\ &+Re\left[\frac{3}{5}\int_R^1 \frac{H_T}{RH^2}\left(\int_0^R R\frac{\partial H}{\partial T}dR\right)dR - \frac{6}{5}\int_R^1 \frac{1}{RH}\frac{\partial}{\partial T}\left(\int_0^R R\frac{\partial H}{\partial T}dR\right)dR\right. \\ &-\frac{54}{35}\int_R^1 \frac{1}{R^3H^2}\left(\int_0^R R\frac{\partial H}{\partial T}dR\right)^2 dR - \frac{54}{35}\int_R^1 \frac{H_R}{R^2H^3}\left(\int_0^R R\frac{\partial H}{\partial T}dR\right)^2 dR \\ &\left.+\frac{81}{35}\int_R^1 \frac{H_T}{RH^2}\left(\int_0^R R\frac{\partial H}{\partial T}dR\right)dR\right]. \end{aligned} \tag{3.4}$$

When $H(R,T)$ is independent of R, the pressure in the curved squeeze film case reduces to that in the flat plate case. The non-dimensional form of the squeeze film force is given by

$$F_{sq} = \int_0^1 R\left(P + (\delta^4 W_R + \delta^2 U_Z)H_R - 2\delta^2 W_Z\right)|_{Z=H(R,T)}dR, \tag{3.5}$$

where $F_{sq} = \frac{f_{sq}h_0^2}{2\pi\mu\omega r_a^4}$, $\delta = \frac{h_0}{r_a}$ and f_{sq} is the dimensional squeeze film force obtained by integrating pressure.

Using equations (3.2), (3.3) and (3.4) in equation (3.5), the squeeze film force for an arbitrary shape of the upper curved disk can be obtained. Using the continuity equation (2.1) in equation (2.4) and integrating with respect to Z from $Z = 0$ to $Z = H(R,T)$, the energy equation is given by

$$\begin{aligned} RePr&\left(\frac{\partial}{\partial T}\int_0^H \Theta dZ + \frac{\partial}{\partial R}\int_0^H (U\Theta)dZ + \frac{\partial}{\partial Z}\int_0^H (W\Theta)dZ + \int_0^H \left(\frac{U\Theta}{R}\right)dZ\right) \\ &= \int_0^H \frac{\partial^2\Theta}{\partial Z^2}dZ + EcPr\int_0^H \left(\frac{\partial U}{\partial Z}\right)^2 dZ. \end{aligned} \tag{3.6}$$

Assuming that the temperature variation in Z-direction is small in equation (2.4), the convective term is taken as constant in the Z-direction and it is denoted by M as

$$\frac{\partial^2\Theta}{\partial Z^2} + EcPr\left(\frac{\partial U}{\partial Z}\right)^2 = M. \tag{3.7}$$

Using equation (3.2) and integrating equation (3.7) twice with respect to Z with the boundary conditions (2.7) and (2.8), the temperature Θ in terms of M is obtained as

$$\Theta = M\left(\frac{Z^2}{2} - HZ\right) + 1 - EcPr\left(\frac{36}{R^2H^6}\left(\int_0^R R\frac{\partial H}{\partial T}dR\right)^2\right)\left(\frac{Z^4}{3} + \frac{H^2Z^2}{2} - \frac{2HZ^3}{3} - \frac{H^3Z}{3}\right). \tag{3.8}$$

Using equation (3.8) in equation (3.6) together with the boundary condition (2.8) and $\frac{\partial\Theta}{\partial Z} = Nu$ at $Z = 0$, the convective term M in equation (3.8) is obtained as

$$M = \frac{M_1}{M_2}, \tag{3.9}$$

where

$$M_1 = \frac{Nu}{RePr} + \frac{Ec}{Re}\left(\frac{12}{R^2H^3}\left(\int_0^R R\frac{\partial H}{\partial T}dR\right)^2\right)$$

$$+\frac{18}{5}PrEc\left(\frac{H_T}{R^2H^2}\left(\int_0^R R\frac{\partial H}{\partial T}dR\right)^2-\frac{1}{R^2H}\frac{\partial}{\partial T}\left(\int_0^R R\frac{\partial H}{\partial T}dR\right)^2\right)+\frac{129}{35}PrEc$$
$$\cdot\left(\left(\frac{-2}{R^4H^2}\left(\int_0^R R\frac{\partial H}{\partial T}dR\right)^3\right)-\left(\frac{2}{R^3H^3}\left(\int_0^R R\frac{\partial H}{\partial T}dR\right)^3\right)+\left(\frac{3H_T}{R^2H^2}\left(\int_0^R R\frac{\partial H}{\partial T}dR\right)^2\right)\right)$$

and

$$M_2=\frac{7HH_R}{10R}\left(\int_0^R R\frac{\partial H}{\partial T}dR\right)-\frac{13H^2H_T}{20}.$$

The temperature expression is obtained by using equation (3.9) in equation (3.8). Finally, using this temperature expression into equation (2.10), the mean temperature is obtained as

$$\Theta_m=\frac{M_1}{M_2}\left(\frac{-H^2}{3}\right)+\frac{18}{5}\frac{EcPr}{R^2H^2}\left(\int_0^R\frac{dH}{dT}dR\right)^2+1. \tag{3.10}$$

The curvature effects of upper disk on the squeeze film characteristics are examined for an exponential form of the gapwidth $h(r,t)=h_1(t)\widehat{k}(r)$ [7]. Here, $h(r,t)$ is taken as a product of volumetric central film thickness $h_1(t)$ and a curvature profile of the curved disk $\widehat{k}(r)$ where $\widehat{k}(r)$ is taken as $e^{-\widehat{c}r^2}$, $\widehat{c}$ is the curvature parameter with $\widehat{c}>0$ for concave disk and $\widehat{c}<0$ for convex disk. The motion of the upper curved disk can be treated as sinusoidal, given by $h_1(t)=h_{10}+e\sin\omega t$, where e is the amplitude, and ω is the angular frequency of the sinusoidal motion. In this case, the characteristic length h_0 in the axial direction is taken as theinitial central film thickness h_{10}.

Using the non-dimensional quantities from equation (2.11) and

$$H_1=\frac{h_1}{h_{10}},\quad E=\frac{e}{h_{10}} \tag{3.11}$$

the dimensionless form of $h(r,t)$ taking $C=\widehat{c}r_a^2$ is given by

$$H(R,T)=H_1(T)K(R)=(1+E\sin T)e^{-CR^2}. \tag{3.12}$$

The non-dimensional pressure, force and mean temperature expressions in this case are obtained from equations (3.4), (3.5) and (3.10), respectively as

$$P=\frac{-6\dot{H}_1}{H_1^3}\int_R^1\frac{R}{K^3}dR+Re\left(\frac{15}{14}\left(\frac{\dot{H}_1}{H_1}\right)^2\int_R^1\frac{R}{K^2}dR-\frac{3}{5}\frac{\ddot{H}_1}{H_1}\int_R^1\frac{R}{K}dR-\frac{27}{70}\left(\frac{\dot{H}_1}{H_1}\right)^2\int_R^1\frac{R^2}{K^3}\frac{dK}{dR}dR\right), \tag{3.13}$$

$$\begin{aligned}F_{sq}=&\int_0^1 R\left[\frac{-6\dot{H}_1}{H_1^3}dR+Re\left(\frac{15}{14}\left(\frac{\dot{H}_1}{H_1}\right)^2\int_R^1\frac{R}{K^2}dR-\frac{3}{5}\frac{\ddot{H}_1}{H_1}\int_R^1\frac{R}{K}dR-\frac{27}{70}\left(\frac{\dot{H}_1}{H_1}\right)^2\int_R^1\frac{R^2}{K^3}\frac{dK}{dR}dR\right)\right.\\&+\delta^4\left[-\frac{9}{K^2}\left(\frac{dK}{dR}\right)^2+\frac{R}{K^3}\frac{3R^3\dot{H}_1H_1^{12}K^{11}}{2}\frac{dK}{dR}+\frac{3R^4\dot{H}_1H_1^{12}K^{10}}{2}\left(\frac{dK}{dR}\right)^2+\frac{3\dot{H}_1}{2K}\frac{d^2K}{dR^2}\right.\\&\left.\left.-\frac{3R^3\dot{H}_1H_1^9K^8}{2}\frac{dK}{dR}+\frac{3\dot{H}_1R}{2K}\frac{d^2K}{dR^2}-\frac{9R^4\dot{H}_1H_1^6K^4}{2}\left(\frac{dK}{dR}\right)^2\right]-\frac{3\delta^2R\dot{H}_1}{H_1K^2}\frac{dK}{dR}\right]dR,\end{aligned} \tag{3.14}$$

$$\Theta_m=\frac{\Theta_{m_1}}{\Theta_{m_2}}\left(-\frac{(H_1K)^2}{3}\right)+\frac{9}{10}PrEc\frac{R^2(\dot{H}_1)^2}{(H_1K)^2}+1, \tag{3.15}$$

where

$$\Theta_{m_1}=\frac{Nu}{RePr}+\frac{Ec}{Re}\left(\frac{3R^2(\dot{H}_1)^2}{(H_1K)^3}\right)+PrEc\left(\frac{96R^2(\dot{H}_1)^3}{35(H_1K)^2}-\frac{9R^2\dot{H}_1\ddot{H}_1}{5H_1K}-\frac{129R^3(\dot{H}_1)^3}{140(H_1K)^3}\right)$$

and

$$\Theta_{m_2} = \frac{7RH_1^2\dot{H}_1K}{20}\frac{dK}{dR} - \frac{13(H_1K)^2\dot{H}_1}{20}.$$

Here, dot (•) represents differentiation with respect to T. Integration of pressure and force expressions are difficult to evaluate analytically and so they are obtained numerically by using adaptive Simpson's rule.

The mean temperature of equation (3.15) is evaluated for two different types of nanofluids namely (i) Copper water nanofluid and (ii) Alumina water nanofluid [1, 5]. Water is taken as the base fluid for both types of nanofluids with base temperature 293 K and Prandtl number $Pr = 7.02$. The diameter of solid spherical copper water nanoparticle is taken as 100 nm. The calculations of thermal conductivity for alumina (Aluminium oxide) water nanofluid and copper water nanofluid with spherical shape of nanoparticles are presented [6, 9]. The thermal properties of all nanofluids depend on the volume fraction ϕ of the nanoparticles. The effective density, heat capacity, dynamic viscosity and thermal conductivity of nanofluids are presented in literature [2, 3].

$$\rho_{nf} = (1-\phi)\rho_{bf} + \phi\rho_s, \tag{3.16}$$

$$(\rho C_p)_{nf} = (1-\phi)(\rho C_P)_{bf} + \phi(\rho C_p)_s, \tag{3.17}$$

$$\mu_{nf} = \frac{\mu_{bf}}{(1-\phi)^{2.5}}, \tag{3.18}$$

$$k_{nf} = k_{bf}\left\{\frac{(k_s/k_{bf}) + (n-1) - (n-1)\phi(1-(k_s/k_{bf}))}{(k_s/k_{bf}) + (n-1) + \phi(1-(k_s/k_{bf}))}\right\}, \tag{3.19}$$

where n is the empirical shape factor of nanofluid and in equations (3.16)-(3.19), the subscripts 'nf', 'bf' and 's' represent the properties of nanofluid, base fluid and nanoparticles respectively. The density ρ (Kg/m^3), specific heat capacity C_p (J/KgK) and thermal conductivity k (W/mK) at 20° C, respectively of the base fluid water are 1000.52, 4181.8 and 0.597, and those of copper are 8954, 383.1 and 386, and those of alumina are 3970, 769 and 36.

4. Results and Discussion

Inertial, thermal and curvature effects on the squeeze film behaviour between a flat circular stationary disk and a curved circular moving disk are investigated using energy integral method. The non-dimensional squeeze film pressure from equation (3.13) and load carrying capacity from equation (3.14) are obtained for the gapwidth given by equation (3.12). The mean temperature distribution of copper water and alumina water nanofluids with different volume fractions are obtained using the thermal physical properties of nanofluids and Eq. (3.15). The value of the local heat transfer coefficient is $Nu = 0.332(Re)^{0.5}(Pr)^{0.333}$. Further, in all these graphs, solid lines correspond to a concave disk, dashed lines correspond to a convex disk and dash dotted lines correspond to the flat disk case.

In Figures 2-10, the characteristic time T is taken as 0.8 and amplitude E is taken as 0.2 or 0.4. Figure 2 shows the radial pressure distribution in the case of concave disk $C > 0$ and convex disk $C < 0$. Figures 3-5 give the force distribution as a function of time. Figures 3 and 4 show the curvature effects on the force distribution in the case of concave disk $C > 0$ and convex disk $C < 0$, respectively. Figure 5 shows the force distribution in the case of different values of

Reynolds number with concave and convex disks. The temperature profiles have been plotted in Figures 6-10 and the values of various parameters are used for copper water and alumina water nanofluids [1, 5]. Figures 6-9 correspond to the mean temperature profile for copper water nanofluid and Figure 10 corresponds to the mean temperature profile for alumina water nanofluid. Figures 6 and 7 respectively show the mean temperature distribution of concave disk $C > 0$ and convex disk $C < 0$ for different Reynolds numbers (Re) with different volume fractions ϕ and a fixed Eckert number (Ec) taken as 0.01. Figure 8 shows the mean temperature distribution of concave disk $C > 0$ and convex disk $C < 0$ for different Re with different Ec and volume fraction $\phi = 0.09$ ($Pr = 2.60$). Figures 9 and 10 respectively show the mean temperature distribution of copper water and alumina water nanofluids for concave, flat and convex disks with particular volume fraction.

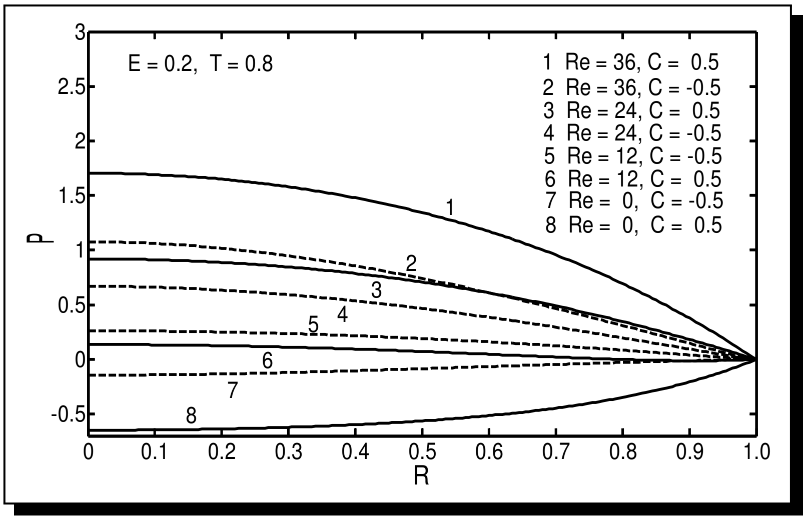

Figure 2. Inertial effects on radial pressure distribution (concave and convex disks)

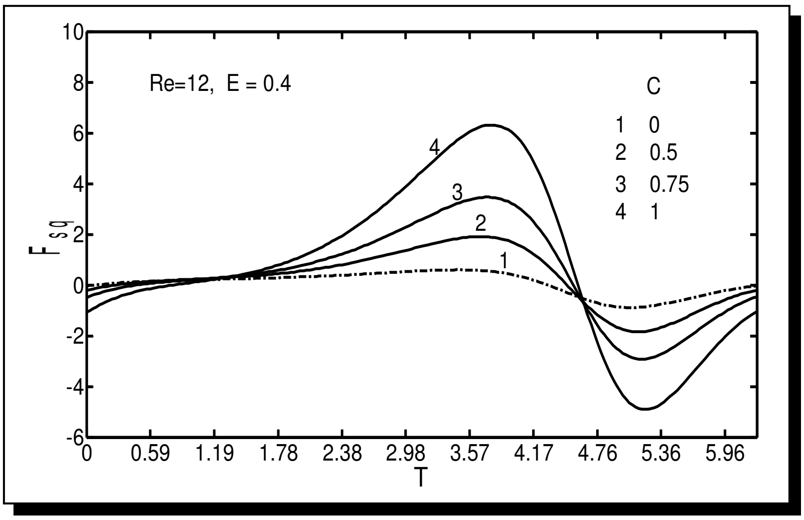

Figure 3. Curvature effects on squeeze film force distribution (concave disk)

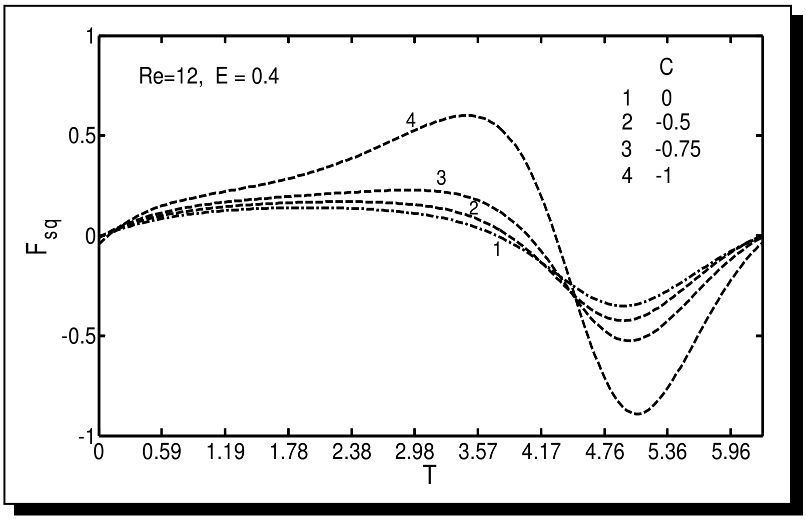

Figure 4. Curvature effects on squeeze film force distribution (convex disk)

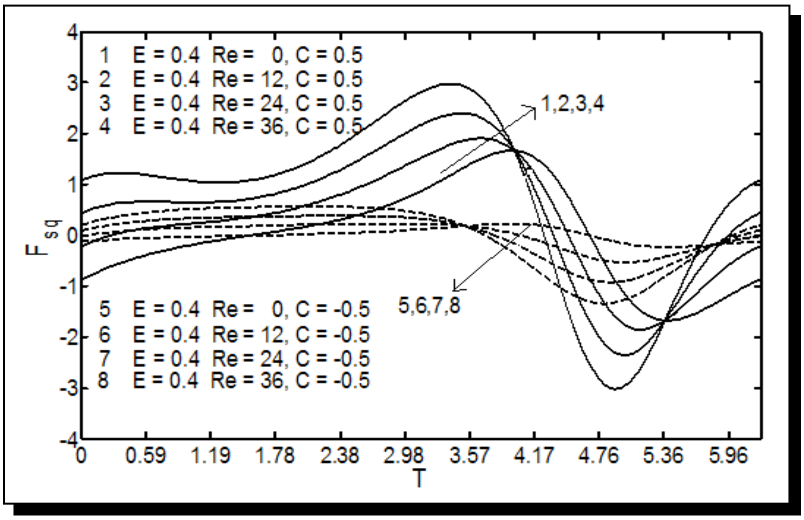

Figure 5. Inertial effects on squeeze film force distribution

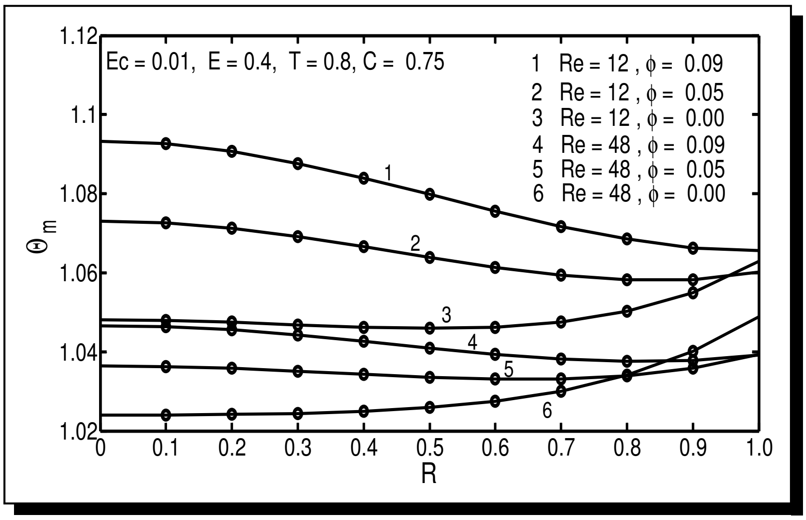

Figure 6. Effects of volume fraction on temperature profile (concave disk) of copper water nanofluid (∘∘∘ numerical solution, — analytical solution)

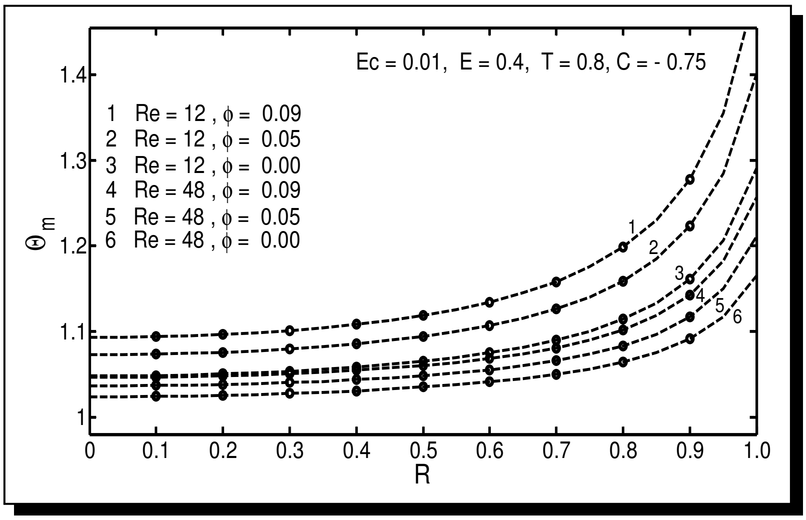

Figure 7. Effects of volume fraction on temperature profile (convex disk) of copper water nanofluid (○○○ numerical solution, - - - analytical solution)

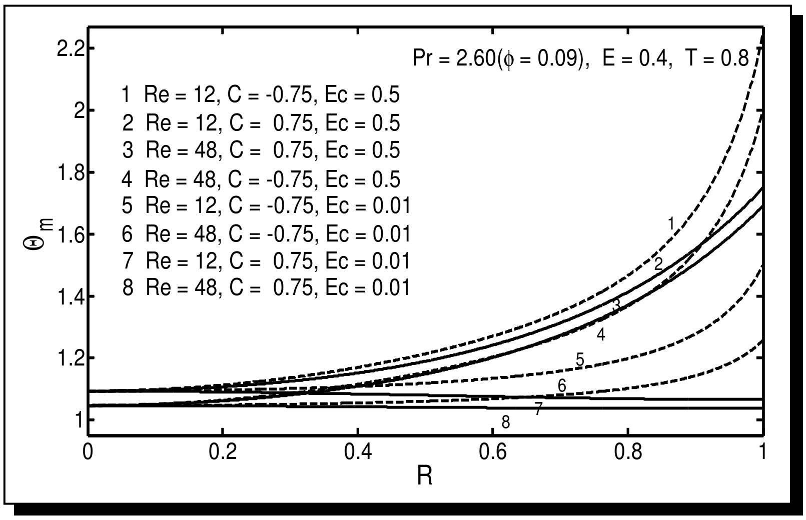

Figure 8. Effects of Ec on temperature profile of copper water nanofluid

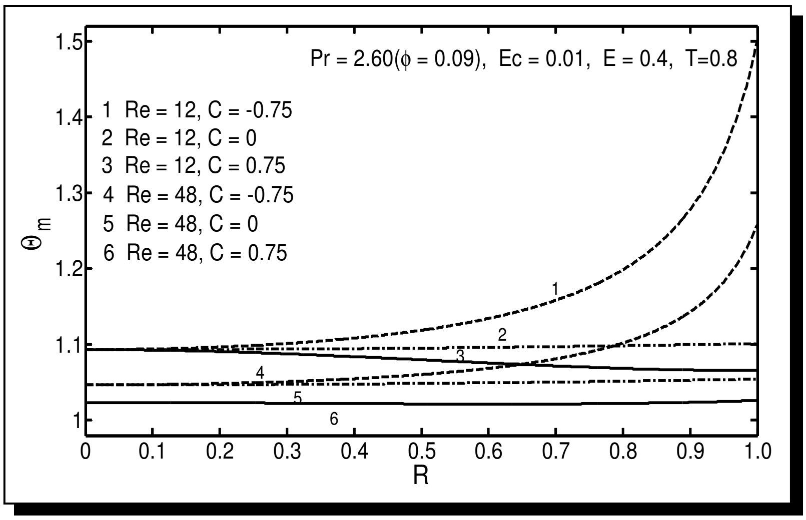

Figure 9. Curvature effects on temperature profile of copper water nanofluid

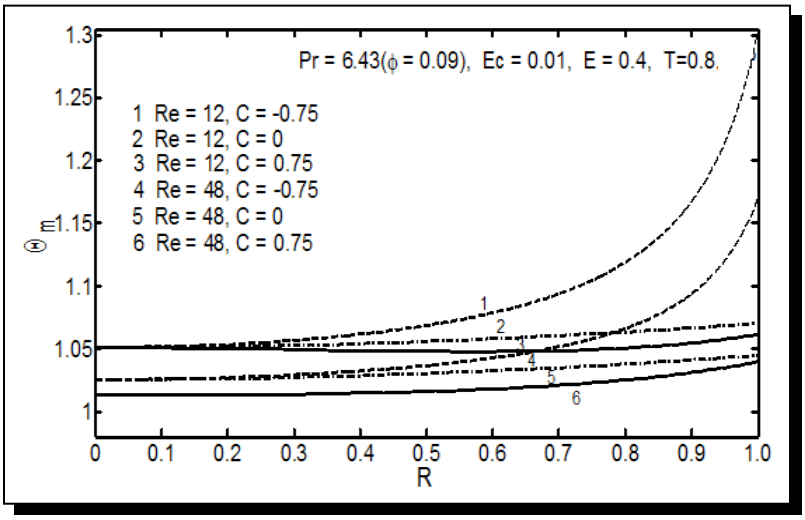

Figure 10. Curvature effects on temperature profile of alumina water nanofluid

The following observations are made from these graphs:

- the radial pressure distribution increases with an increase in Re;
- squeeze film force increases with an increase in concave nature of the curved disk and with an increase in Re;
- mean temperature decreases with an increase in Re for various volume fractions, whereas it increases with an increase in Ec;
- as far as squeeze film pressure and force are concerned the concave nature and high inertial effects of the upper disk seem favourable. However, the mean transfer distribution is better for convex nature of the upper disk and low inertia cases;
- the mean temperature increase is more significant for copper water nanofluid than alumina water nanofluid for all the cases because of the effective thermal properties of copper water nanofluid.

5. Conclusion

The laminar flow of an incompressible viscous nanofluid between a flat circular stationary disk and an axisymmetric curved circular moving disk is examined using energy integral method. The combined inertial and curvature effects are considered. Here, one wall is taken to satisfy the isothermal condition and the other is taken to satisfy the adiabatic condition. The squeeze film pressure, load carrying capacity and mean temperature of the copper water and alumina water nanofluids are investigated for an exponential form of the gapwidth. The increasing inertial effect is more significant for increasing load carrying capacity and increasing heat transfer rate. In the case of high inertial effect the convection is more dominant. Therefore the moderate inertial effect is more significant for nanofluid lubrication.

Competing Interests

The authors declare that they have no competing interests.

Authors' Contributions

All the authors contributed significantly in writing this article. The authors read and approved the final manuscript.

References

[1] S.P. Anjali Devi and A. Julie, Laminar boundary layer flow of nanofluid over a flat plate, *Int. J. of Appl. Math & Mech.* **7**(6) (2011), 52 – 71.

[2] H.C. Brinkman, The viscosity of concentrated suspensions and solutions, *The J. Chemical Phys.* **20**(4) (1952), 571 – 581.

[3] J. Buongiorno, Convective transport in nanofluids, *Transactions of the ASME* **128** (2006), 240 – 250.

[4] H.M. Duwairi, B. Tashtoush and R.A. Damseh, On heat transfer effects of a viscous fluid squeezed and extruded between two parallel plates, *Heat Mass Transfer* **41** (2004), 112 – 117.

[5] K. Gangadhar, Radiation and viscous dissipation effects on laminar boundary layer flow nanofluid over a vertical plate with a convective surface boundary condition with suction, *J. Applied Fluid Mech.* **9**(4) (2015), 2097 – 2103.

[6] L. Gosselin and A.K. Silva, Combined "heat transfer and power dissipation" optimization of nanofluid flows, *Applied Physics Letters* **85**(18) (2004), 4160 – 4162.

[7] R.S. Gupta and V.K. Kapur, The simultaneous effects of thermal and inertial in curved circular squeeze films, *J. Lubrication Tech.* **102** (1980), 501 – 504.

[8] M.M. Hashmi, T. Hayat and A. Alsaedi, On the analytic solutions for squeezing flow of nanofluid between parallel disks, *Nonlinear Analysis: Modelling and Control* **17**(4) (2012), 418 – 430.

[9] H.E. Patel, T. Pradeep, T. Sundararajan, A. Dasgupta, N. Dasgupta and S.K. Das, A micro-convection model for thermal conductivity of nanofluids, *Pramana – J. of Phys*. **65**(5) (2005), 863 – 869.

[10] D.P. Prasad, P. Singh and P. Sinha, Thermal and inertial effects in rollers with power law lubricant having temperature and pressure dependent consistency, *Indian J. Pure Appl. Math*. **23**(4) (1992), 305 – 320.

[11] R. Usha and P. Vimala, Inertial effects in a curved non-Newtonian squeeze film, *ASME Trans. J. Trib.* **68** (2001), 944 – 948.

[12] R. Usha and P. Vimala, Curved squeeze film with inertial effects – energy integral approach, *Fluid Dyn. Res.* **30** (2002), 139 – 153.

[13] R. Usha and P. Vimala, Theoretical investigation of unsteady squeeze flow in curved Newtonian squeeze film, *ASME Trans. J. Trib.* **124** (2002), 865 – 869.

[14] M. Vimala and G. Sumathi, Theoretical investigation of couple stress squeeze films in a curved circular geometry, *ASME Trans. J. Trib.* **133** (2011), 041701-1–041701-8.